A study of structural, magnetic and optical properties of $Zn_{1-x}Cr_xO$

SHI FENG NIU*, JIA HONG ZHENG[a, b]
College Key laboratory automotive transportaion safety technology ministry of communication, chang'an university, xi'an, 710064, shaanxi, P. R. China
[a]*College of Materials Science and Engineering, Nanling campus, Jilin University, Changchun, 130022, Jilin, P. R. China*
[b]*Key Laboratory of Preparation and Applications of Environmental Friendly Materials, Jilin Normal University, Chinese Ministry of Education, Siping 136000, China*

Cr-doped ZnO powders were synthesized successfully with different doping concentration by sol–gel method. The structural, optical and magnetic properties of the samples were investigated by X-ray diffraction (XRD), X-ray photoelectron spectroscopy (XPS), photoluminescence (PL) and vibrating sample magnetometer (VSM). XRD and XPS indicate that the Cr ions are at least partially substitutionally incorporated into the crystal lattice of ZnO. The saturation doping concentration of Cr in ZnO lattice is estimated to be less than 7.0 at %. Magnetic measurements indicated that the Cr-doped ZnO samples show ferromagnetic behavior at room temperature and the ferromagnetism decreases with increasing Cr doping concentration. PL measurements showed that $Zn_{1-x}Cr_xO$ powders with the increased of Cr concentration exhibited obvious blue shift and the intensity of the green emission band is enhanced.

(Received July 2, 2012; accepted February 20; 2013)

Keywords: Diluted magnetic semiconductors, Ferromagnetism, Optical properties

1. Introduction

Diluted magnetic semiconductors (DMSs) have attracted considerable attention by the partial replacement of cations in a non-magnetic semiconductor and by magnetic transition metal ions for spintronic applications. For practical spintronic devices, it is necessary to develop semiconducting materials that show ferromagnetic behavior at room temperature. The main efforts in DMS research are focused on doping non-magnetic semiconductors with transition metals (TM), including TM-doped III–V [1], II–VI [2] or group IV types [3]. However, most DMSs have low Curie temperature, which limits their practical applications. Nowadays, extensive efforts have been made to study wide-band-gap oxide/nitride DMSs, such as the transition metal doped ZnO, TiO_2, SnO_2, In_2O_3 and GaN [4–5]. Among them, ZnO with a wide band gap energy (E_g = 3.37eV) and a relatively large exciton binding energy (60 meV) at room temperature, has good photoelectric and piezoelectric characteristics [6,7]. In the quest for materials with a high transition temperature, transition metal (TM)-doped ZnO has emerged as an attractive candidate according to both theoretical and experimental studies. Both experimental results and theoretical calculations revealed that V, Cr, Fe, Co and Ni doped ZnO exhibits ferromagnetism ordering above the room temperature [8-11]. A drawback of this approach is that the dopant material can segregate to form precipitates or clusters that are actually responsible for the ferromagnetic properties.

Among these dopant elements, Cr-doped ZnO has many advantages. Cr is antiferromagnetic, thus its possible presence in the form of segregated clusters or compounds (expect nanocrystalline CrO_2) would not contribute to ferromagnetism. The radius of Zn^{2+} is around 15 % only higher than Cr^{3+}, making Cr a favorable dopant. In particular, trivalent Cr^{3+} ions exhibit $3d^3$ high-spin configuration, which may help to generate large magnetic moments in the host semiconductors [12]. These features make Cr a promising dopant to distinguish intrinsic ferromagnetism from the secondary phases or precipitates in DMSs. Therefore, to some extent, the study of the Cr-doped ZnO DMSs can effectively tell whether the FM originates from the existence of magnetic clustering or not. Until now, most of the studies on the Cr-doped ZnO have focused on the thin film supported by the substrate [13-14]. The reproductive rate of the thin film is low, and the more important fact is that the lattice constant of the substrate does not usually match with that of ZnO, so that will cause the lattice distortion of ZnO [15]. However, compared with the widely studied Co- or Mn-doped ZnO systems, both theoretical and experimental results on Cr-doped ZnO

are scarce. Therefore, in this paper, Cr-doped ZnO nanoparticles were repared via sol-gel method and the effect of Cr concentration on the photoluminescence properties was investigated.

2. Experimental

$Zn_{1-x}Cr_xO$ powders with x = 0.00, 0.03, 0.05, 0.07 and 0.09 at% were prepared via sol-gel method. All the chemical reagents used in the experiment were analytical grade purity. Zinc nitrate [$Zn(NO_3)_2 \cdot 6H_2O$] and different ratios of chromium nitrate [$Cr(NO_3)_2 \cdot 9H_2O$] were dissolved into the citrate acid [$C_6H_8O_7 \cdot H_2O$] solution with stirring to form sol. Then, the mixture was polymerized to form gel. The swelled gel was pyrolyzed at 130 °C to obtain the reticular precursor. The precursor was further ground into powders in an agate mortar and then sintered at 400 °C for 3 hours in a box furnace to obtain $Zn_{1-x}Cr_xO$ nanoparticles.

X-ray diffraction was employed to determine the phase structure, performed on a D/max-Rigaku XRD diffraction spectrometer with a Cu Kα line of 1.5417 Å and a monochromator at 50 kV and 300 mA. XPS spectra of the ZnO powders were acquired with an ESCALABMk II (Vacuum Generators) spectrometer using unmonochromatized Al Kα X-rays (240 W). Cycles of XPS measurements were done in a high vacuum chamber with a base pressure of 10^{-8} Torr. The room-temperature PL spectra were measured with a fluorescence spectrophotometer using a He-Cd laser of a wavelength of 325 nm as the excitation light source.

3. Results and discussion

The XRD patterns and the change in the lattice constants of as-synthesized ZnO samples with different concentration of Cr ions doping (x=0.00, 0.01, 0.03, 0.05, and 0.07) are shown in Fig. 1. As can be seen from Fig. 1 (a), there are no Cr metal or the Cr oxides impurity phases are found and all diffraction peaks could be indexed to wurtzite hexagonal ZnO (JCPDS Card No. 36-1451). However, for x=0.07 in the Fig. 1 (b), the secondary phase of $ZnCr_2O_4$ emerges, so the limit concentration of Cr doping into ZnO lattice should be less than 7 at %. Fig. 1(c) shows the variation of the lattice constant a and c as the function of Cr content in the sample. The decrease in a and c axis lattice constant with increasing Cr concentration indicates the contraction of lattice distance due to the doping of small sized Cr atoms into the ZnO lattice, as the ionic radius of Cr (0.063 nm) is much smaller than that of Zn (0.074 nm). That justifies the considerable lattice contraction.

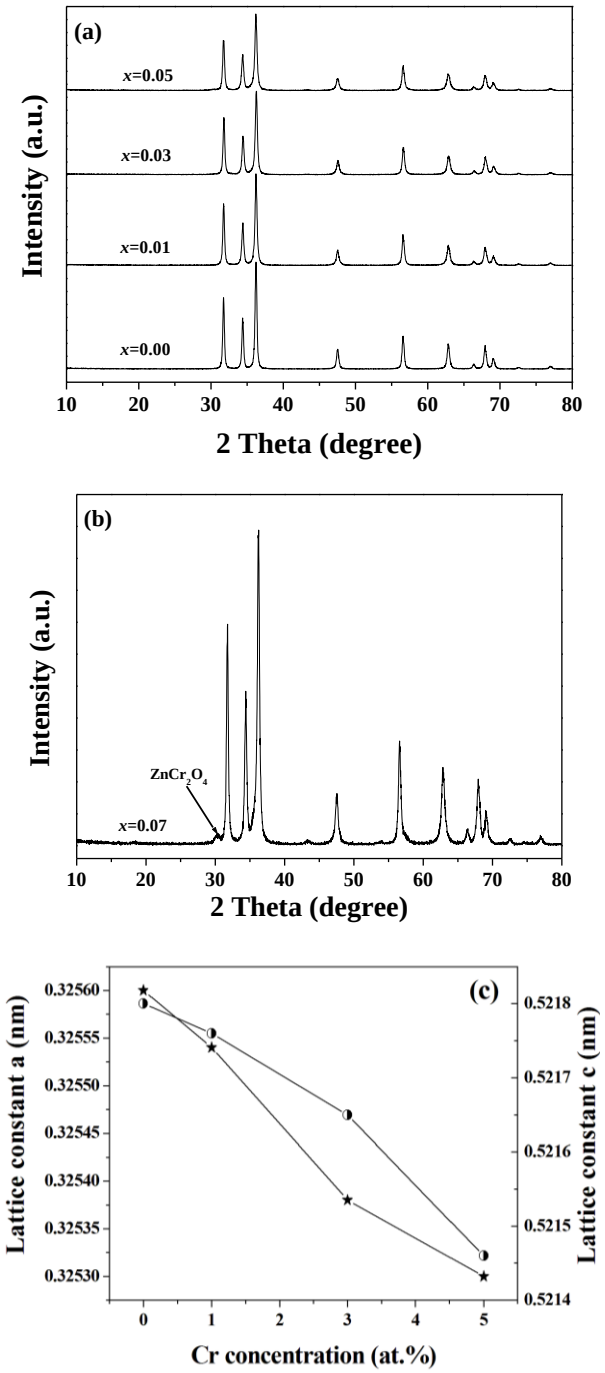

Fig. 1. (a) XRD patterns of $Zn_{1-x}Cr_xO$ nanoparticals with different concentrations (x = 0.00, 0.01, 0.03, 0.05), (b) x = 0.07,and (c) the change in the lattice constants a and c.

The average grain size (D) of the samples was estimated with the help of Scherrer equation using the diffraction intensity of (101) peak $D = 0.89\lambda / \beta \cos\theta$, where D is the crystallite size, λ is the X-ray wavelength,

θ is the Bragg diffraction angle and β is the peak full width at half maximum (FWHM) of the ZnO (101) line. The calculated average grain sizes of $Zn_{1-x}Cr_xO$ (x=0.00, 0.01, 0.03, 0.05, and 0.07) are 41.1 nm, 38.9 nm, 34.5 nm, 32.8 nm, and 30.1 nm, respectively. The reduce of grain size has two reasons. 1, the doping of smaller radius of Cr^{3+} ions (0.063 nm) than that of Zn^{2+} ions (0.074 nm) into ZnO lattice. Once Cr^{3+} ions replace Zn^{2+}, the bonding length of Cr-O will be shorter in comparison with Zn-O. Therefore, the grain sizes will decrease. 2, the doping of Cr^{3+} ions into ZnO lattice restrains crystalline grain from growing up.

In order to determine the chemical states of Cr in the as-synthesized nanopowders, the XPS spectra of $Zn_{0.95}Cr_{0.05}O$ are shown in Fig. 2. Fig. 2(a) depicts the XPS survey spectrum, in which all the peaks of Zn, Cr, O and C elements are labeled, with the adventitious carbon C 1s peak at 285.0 eV being used as reference for calibrating the binding energy. Fig. 2(b) shows the XPS spectrum of Zn 2p in the Cr doped ZnO particles. The binding energy of Zn $2p_{3/2}$ and Zn $2p_{1/2}$ locates at 1021.2 eV and 1045.6 eV, respectively, and the peak separation between them is 24.5 eV, which is well located in the range of the standard reference value of ZnO [16]. It indicates that the majority of Zn ions mainly exist in the lattice of zinc oxide [17]. As shown in Fig. 2 (c), for $Zn_{0.95}Cr_{0.05}O$ sample, the Cr 2p level is split into a doublet with an energy separation due to the spin-orbit interaction [18]. The peak of Cr $2p_{3/2}$ is detected at 576.6 eV for the sample. The positions of the peak is clearly different from 574.0 eV of Cr metal and 576.0 eV of Cr^{2+} [19-21] which match well with the reported binding energy 576.7±.2 eV of the $2p_{3/2}$ level of Cr^{3+} states [19-22]. Moreover, the Cr $2p_{1/2}$ peak located at 585.8 eV. The intensity of the Cr $2p_{1/2}$ is stronger than that of Cr $2p_{3/2}$. The main reason is that the overlap of the XPS photoelectron of Cr $2p_{1/2}$ located at 585.2 eV and the Auger electron peak of Zn located at 585.0 eV leads to the phenomenon [23]. In order to indicate the evolution with composition of Cr 2p splitting, the XPS spectra of Cr for $Zn_{0.97}Cr_{0.03}O$ was also been given in the Fig. 2 (c). As shown in Fig. 2 (c), we can find that the f Cr $2p_{3/2}$ peak position for $Zn_{0.97}Cr_{0.03}O$ sample is located at 576.4 eV, the peak position is quite close to the peak position of Cr $2p_{3/2}$ in Cr^{3+} states. It further suggests that Cr ions are actually incorporated into the ZnO lattice as Cr^{3+} ions. That is to say, the decrease of Cr doping concentration in ZnO sample does not change the valence state of Cr. According to the Fig. 1 (c) result, with decreasing Cr doping concentration, the lattice parameters increase, which will make the binding energy of Cr 2p decrease. This result clearly shows that Cr has been incorporated as Cr^{3+} in ZnO lattice.

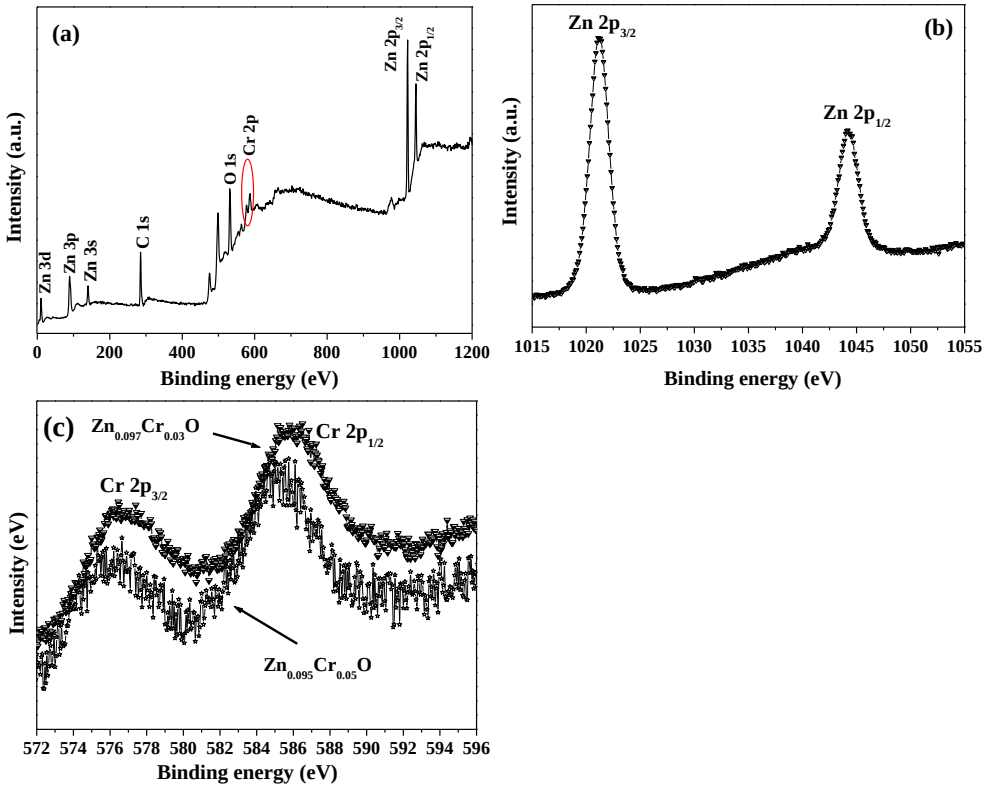

Fig. 2. XPS spectra of Cr doped ZnO nanoparticals for $Zn_{0.95}Cr_{0.05}O$ (a), Zn 2p for $Zn_{0.95}Cr_{0.05}O$ (b), and Cr 2p for $Zn_{0.95}Cr_{0.05}O$ and $Zn_{0.97}Cr_{0.03}O$ (c).

Magnetic measurements on $Zn_{1-x}Cr_xO$ were performed using VSM. Fig. 3 shows the dependence of magnetic field (H) on the magnetization (M) at room temperature for $Zn_{1-x}Cr_xO$ (x=0.01,0.03,0.05) powders with different Cr concentrations. All three loops are found to be hysteretic as shown in Fig. 3, indicating ferromagnetic behavior at room temperature. The 1.0, 3.0 and 5.0 at.% Cr-doped samples possess the remnant magnetizations of ~ 0.023, ~0.013 and ~0.023 emu/g, respectively. The ferromagnetism decreases with increasing Cr concentration, and the $Zn_{1-x}Cu_xO$ alloy with x = 0.05 possesses the largest saturated magnetization. In principle, as the Cr concentration in ZnO samples increases, a number of antiferromagnetic phases may occur such as Cr metal, Cr_2O_3 and Cr_3O_4 [24]. However, neither CrO_2 nor other phases (antiferromagnetic Cr metal, Cr_2O_3 and Cr_3O_4) are detected via XRD. Indeed, the sensitivity of XRD may not be the best to identify the minute amounts of second phases in the samples. It is fortunate that these phases (Cr metal, Cr_2O_3 and Cr_3O_4) can be present in small quantities, FM should not be related to these phases because their Neel temperature are below the room temperature. The stronger ferromagnetic behavior in samples with lower concentrations of Cr and its apparent weakening and subsequent disappearance at higher doping concentrations also confirm the absence of the ferromagnetic CrO_2. In addition, CrO_2 is metastable, it is unlikely to form under the low oxygen pressure conditions usually employed in vaccum deposition technique [25]. As is discussed above, the observed FM is not from the secondary phases. We conclude that FM of the $Zn_{1-x}Cr_xO$ in this study is an intrinsic property of the Cr-doped ZnO.

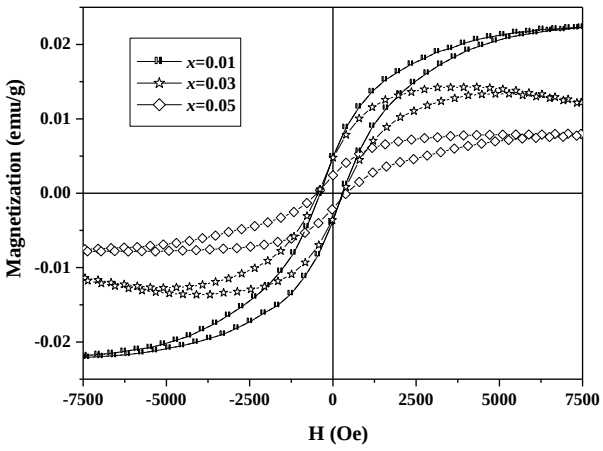

Fig. 3. Magnetic field dependence of magnetization for $Zn_{1-x}Cr_xO$ (x=0.01, 0.03, 0.05) samples.

Magnetization versus temperature (M–T) curves was also measured in Fig. 4. As seen from this figure, the temperature dependence of the magnetization for $Zn_{0.95}Cr_{0.05}O$ sample is linear at high temperatures. At lower temperatures it displays a steep rise with pronounced concave curvature but without showing any distinct magnetic phase transition. Based on these data we can conclude that the Curie temperature for this sample is well above room temperature, but it is hard to determine the exact value, since the value of the Curie temperature is rather high, exceeding the range of our measurements. Quite a number of works in the literature are shown that Cr-doped ZnO shows ferromagnetism at Curie temperatures above room temperature [26,27].

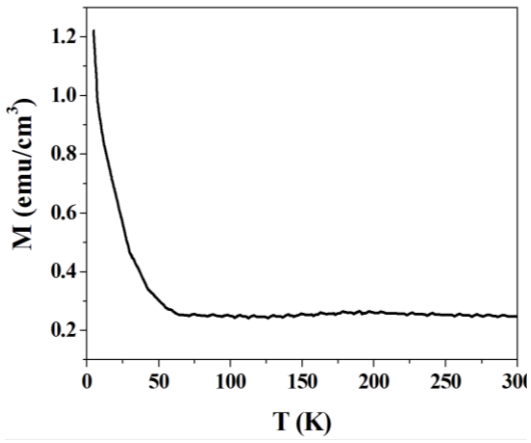

Fig. 4. Temperature dependence of magnetization of $Zn_{1-x}Cr_xO$ (x=0.05) sample.

In order to study the effect of Cr doping concentration on the optical properties of $Zn_{1-x}Cr_xO$ (x=0.01, 0.03, 0.05) samples, PL spectra are shown in Fig. 5. We can observe that all the spectra contain a strong UV band peak around 380 nm, which commonly originates from excitonic recombination corresponding to the near-band-edgeemission of ZnO [28, 29]. It can be seen from Fig. 5 that the UV emission peak position of the Cr-doped ZnO nanoparticle exhibits blue shift with the increase of Cr concentration. The UV emission band is sharply suppressed as well. This indicates that the Cr doping prompts the nonradiative recombination process and that the existence of the transition metal ions like Cr can control the excitonic recombination radiation. In addition, with the increase of Cr doping concentration from x=0.01 to 0.05, the intensity of the green emission band is enhanced. The green emission peak is commonly referred as deep-level or trap state emission [30, 31]. Various mechanisms have been proposed for the green emission of ZnO [32]. Oxygen vacancy was recently testified to be one of the origins of green emission in ZnO, which occurs in three different charge states: the neutral oxygen vacancy (Vo), the singly ionized oxygen vacancy (Vo•), and the doubly ionized oxygen vacancy (Vo••) [33]. The enhanced intensity of the green emission indicates that the density of defects increases, which could be attributed to Cr doping since Cr ions exist in the ZnO crystal lattices with +3

valence stateas discussed in XPS spectra. With increasing the Cr doping concentration, more oxygen vacancies will be introduced in the samples, which finally results in an enhanced green emission in $Zn_{1-x}Cr_xO$ powders [34].

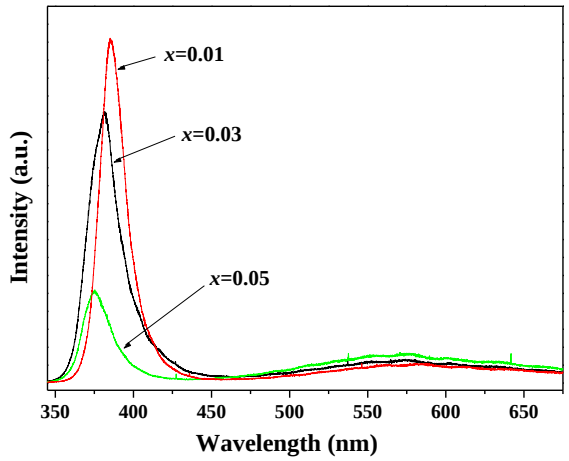

Fig. 5. PL spectra of $Zn_{1-x}Cr_xO$ (x=0.01, 0.03, 0.05) samples.

4. Conclusions

In this letter, the Cr-doped zinc oxide diluted magnetic semiconductors have been synthesized successfully by the sol-gel method. The results indicate that Cr ions were successfully incorporated into ZnO lattice, testified by XRD and XPS spectra. XRD results indicate that the saturation doping concentration of Cr in ZnO lattice is less than 7.0 at %. Room-temperature FM was observed in $Zn_{1-x}Cr_xO$ powers prepared by VSM. The ferromagnetism decreases with increasing Cr doping concentration and the $Zn_{1-x}Cu_xO$ alloy with x = 0.05 possesses the largest saturated magnetization. The UV emission peak position of the Cr-doped ZnO alloy exhibits blue shift and the intensity of green emission is enhanced.with the increase of Cr concentration.

Acknowledgements

The Project was Supported by the Special Fund for Basic Scientific Research of Central Colleges, Chang'an University (NO.CHD2011JC176), Graduate Innovation Fund of Jilin University (No. 20121098), and the Applications of Environmental Friendly Materials from the Key Laboratory Ministry of Education, Jilin Normal University.

References

[1] T. Jungwirth, J. Sinova, J. Masek, J. Kucera, A. H. MacDonld, Rev. Mod. Phys. **78**, 809 (2006).
[2] S. Delikanli, S. He, Y. Qin, P. Zhang, H. Zeng, H. Zhang, M. Swihart, Appl. Phys. Lett. **93,** 132501 (2008).
[3] Y. D. Park, A. T. Hanbicki, S. C. Erwin, C. S. Hellberg, J. M. Sullivan, J. E. Mattson, T. F. Ambrose, A. Wilson, G. Spanos, B. T. Jonker, Science **295**, 651 (2002).
[4] X. Y. Xu, C. B. Cao, J. Alloys Compd. **501**, 265 (2010).
[5] M. V. Limaye, S. B. Singh, R. Das, P. Poddar, S. K. Kulkarni, J. Solid State Chem. **184,** 391 (2011).
[6] J. H. Lim, C. K. Kang, K. K. Kim, I. K. Park, D. K. Hwang, S. J. Park, Adv. Mater. **18**, 2720 (2006).
[7] J. K. Furdyna, J. Appl. Phys. **64**, R29 (1988).
[8] M. Peiteado, A. C. Caballero, D. Makovec, J. Solid State Chem. **180**, 2459 (2007).
[9] M. Peiteado, D. Makovec, M. Villegas, A. C. Caballero, J. Solid State Chem. **181**, 2456 (2008).
[10] R. Wen, L. Wang, X. Wang, G. H. Yue, Y. Chen, D. L. Peng, J. Alloys Compd. **508**, 370 (2010).
[11] B. Wang, L. D. Tang, J. Q. Qi, H. L. Du, Z. B. Zhang, J. Alloys Compd. **503,** 436 (2010).
[12] L. Schneider, S. V. Zaitsev, W. Jin, A. Kompch, M. Winterer, M. Acet, G. Bacher, Nanotechnology **20**, 135604 (2009).
[13] J. Elanchezhiyan, K. P. Bhuvana, N. Gopalakrishnan, Y. Chang, S. Sivananthan, M. Senthil Kumar, T. Balasubramanian, J. Alloys Compd. **468**, 7 (2009).
[14] N. Al-Hardan, M. J. Abdullah, A. Abdul Aziz, H. Ahmad, Appl. Surf. Sci. **256**, 3468 (2010).
[15] S. Duhalde, M. F. Vignolo, F. Golmar, C. Chiliotte, M. Weissmann, Phys. Rev. B **72**, 161313 (2005).
[16] Y. Wang, L. Sun, L.G. Kong, J. F. Kang, X. Zhang, R. Q. Han, J. Alloys Compd. **423**, 256 (2006).
[17] C. Y. Leunga, A. B. Djurišić, Y. H. Leung, L. Ding, C. L. Yang, W. K. Ge, J. Cryst. Growth **290**, 131 (2006).
[18] K. Jayanthi, S. Chawla, A. G. Joshi, Z. H. Khan, R. K. Kotnala, J. Phys. Chem. C, **114**, 18429 (2010).
[19] C. Xu, M. Hassel, H. Kuhlenbeck, H. J. Freund, Surf. Sci. **23**, 258 (1991).
[20] A. M. Venezia, C. M. Loxon, J. A. Horton, Surf. Sci. **225**, 195 (1990).
[21] A. Maetaki, M. Yamamoto, H. Matsumoto, K. Kishi, Surf. Sci. **445**, 80 (2000).
[22] K. M. Reddy, R. Benson, J. Hays, A. Thurber, M. H. Engelhard, V. Shutthanandan, R. Hanson, W. B. Knowlton, A. Punnoose, Sol. Energy Mater. Sol. Cells **91**, 1496 (2007).
[23] P. Prathap, N. Revathi, Y. P. Venkata Subbaiah, K. T. Ramakrishna Reddy, J. Phys.: Condens. Matter **20**, 035205 (2008).
[24] X. H. Chen, H. T. Zhang, C. H. Wang, X. G. Luo, P. H. Li, Appl. Phys. Lett. **81**, 4419 (2002).
[25] Q. Zhao, J. J. Yuan, G. H. Wen, G. T. Zou, J. Magn. Magn. Mater. **320**, 2356 (2008).
[26] Y. Liu, J. Yang, Q. Guan, L. Yang, Y. Zhang, Y. Wang, B. Feng, J. Cao, X. Liu, Y. Yang, M. Wei, J. Alloys Compd. **486**, 835 (2009).

[27] I. Satoh, T. Kobayashi, Appl. Surf. Sci. **216**, 603 (2003).
[28]C. K. Xu, K. K. Yang, Y. Y. Liu, L. W. Huang, H. Lee, J. Cho, H. Wang, J. Phys. Chem. C **112**, 19236 (2008).
[29] J. H. Yang, M. Gao, Y. J. Zhang, L. L. Yang, J. H. Lang, D. D. Wang, Y. X. Wang, H. L. Liu, H. G. Fan, M. B. Wei, F. Z. Liu, Chem. Res. Chin. Univ. **24**, 1005 (2008).
[30] P. Zu, Z. K. Tang, G. K. L. Wong, M. Kawasaki, A. Ohtomo, H. Koinuma, Y. Segawa, Solid State Commun.**103**, 459 (1997).
[31] D. M. Bagnall, Y. F. Chen, M. Y. Shen, Z. Zhu, T. Goto, T. Yao, J. Cryst. Growth **184**, 605 (1998).
[32] L. L. Yang, Q. X. Zhao, M. Willander, J.H. Yang, I. Ivanov, J. Appl. Phys. **105**, 053503 (2009).
[33] W. Li, D. Mao, F. Zhang, X. Wang, X. Liu, S. Zou, Y. Zhu, Q. Li, J. Xu, Nucl. Instrum. Methods: Phys. Res. B **169**, 59 (2000).
[34] K. Samanta, P. Bhattacharya, R. S. Katiyarl, J. Alloys Compd. **105**, 113929 (2009).

*Corresponding author: nsf530@chd.edu.cn